EPJ Web of Conferences **343**, 04002 (2025) https://doi.org/10.1051/epjconf/202534304002
AIMACE-2025

Comparative analysis of TOPSIS and MOORA methods for the selection of heat transfer fluid in PVT based hydrogen production system

S.Senthilraja[1*], R.Gangadevi[1], M. Baskaran[2], C.Jegadhesan[3] and *Manjula* Siriwardhana[4]

[1] Department of Mechatronics Engineering, SRM Institute of Science and Technology, Kanchipuram, India
[2] Department of Mechatronics Engineering, K.S.Rangasamy College of Technology, Tiruchengode, India
[3] Department of Automobile Engineering, Kongu Engineering College, Perundurai, India
[4] National Engineering Research and Development Centre of Sri Lanka, Ekala, Jaela, Sri Lanka
[*] Corresponding Author Email: senthils9@srmist.edu.in

Abstract. Photovoltaic – Thermal (PVT) solar collector based hydrogen production system using different coolants such as water, air, nanofluids etc. to enhance the performance by extracting more heat from PV module. In order to evaluate the effectiveness of a hydrogen generation system based on PVT, an experiment was conducted utilizing various coolants in a laminar flow environment. The experiment was carried out between 8:00 AM and 4:00 PM under varying solar radiation conditions, and the hydrogen yield rate increased by approximately 20.7%, 25.6%, and 29.6% in comparison to the PV-based hydrogen production system. Utilizing an organized multi-criteria decision making (MCDM) strategy is necessary to select the most effective cooling fluid for maximizing performance. This research aims to determine the appropriate heat transfer fluid by using the Technique for Order of Preference by Similarity to Ideal Solution (TOPSIS) and Multi-Objective Optimization technique on the basis of Ratio Analysis (MOORA) methodologies. The findings indicated that around 80% of the rankings achieved in both the TOPSIS and MOORA approaches were identical. Furthermore, the hybrid nanofluid consisting of Al2O3 – CuO particles suspended in water, with a nanoparticle concentration of 0.2%, and subjected to 4 hours of sonication, is considered to be of greater importance compared to other fluids.

1 Introduction

In recent years, nanofluid has emerged as a very promising heat transfer fluid for many applications in the field of heat transfer. There has been a dramatic growth in the number of publications in recent years, confirming to the scholars' extensive work in this area. Nanofluids are made by combining typical heat transfer fluids with metal or metal oxide particles that are on the nanometer scale (1 nm to 100 nm). SUS Choi prepared the first nanofluid during the experimental work, and significant improvements in heat transfer compared to traditional fluids were observed. The addition of nanoparticles has significantly

boosted the thermal conductivity, viscosity, density, and specific heat of the base fluid. Agarwal et al. [1] used a wet chemical approach to synthesise CuO nanoparticles and then investigated their thermal and physical characteristics. The findings of the study revealed that nanofluids composed of water, ethylene glycol, and motor oil exhibited thermal conductivity enhancements of around 40%, 27%, and 19% correspondingly. A numerical study was carried out by Aghanajafi et al. [2] to investigate the heat transfer capabilities of a nanofluid composed of CuO nanoparticles and distilled water. The results of the investigation revealed a noteworthy enhancement in the heat transfer coefficient. Usri et al. [3] conducted an experiment involving the creation of nanofluids by dispersing Al_2O_3 in varying fractions of a water and ethylene glycol combination. Their findings revealed a positive correlation between the volume concentration and temperature of the nanofluids, indicating an increase in thermal conductivity.
According to the findings of an investigation by Zawrah et al. [4] into the stability and electrical characteristics of water-based Al_2O_3 nanofluid with sodium dodecylbenzenesulfonate (SDBS) surfactant, nanofluid with 1% SDBS was the most stable. Furthermore, it was shown that the electrical property was improved up to a volume concentration of 0.2%, after which it declined. Microchannel heat sink (MCHS) heat transfer properties were experimentally investigated by Jung and Park [5]. Based on the findings, Al_2O_3 nanofluid generates around 6.7% higher entropy, which results in a greater transfer of energy from the cavity to the top area. Despite the fact that employing nanofluids with single nanoparticles has significantly improved the thermal characteristics of base fluids, there is still potential for improvement in terms of heat transfer rate. Thus, the scientists have paid their attention hybrid nanofluids by dispersing two distinct nanoparticles across a single fluid. Sahoo and Kumar [6] conducted an experimental investigation to examine the influence of the volume concentration of Al_2O_3 – CuO – TiO_2 / water nanoparticles on viscosity and the findings revealed a significant reduction of 23.64% in dynamic viscosity. Esfe et al. [7] investigated the thermal conductivity of various ratios of MWCNT–MgO/water–EG nanofluids and the results revealed that the nanofluid with a MWCNT:MgO ratio of (90 : 10) exhibited the highest thermal conductivity among the tested nanofluids. Sahoo [8] dispersed Al2O3-SiC-TiO2 nanoparticles in water to create a nanofluid, and then they measured the fluid's viscosity as a function of its concentration in different volumes. According to the data, the viscosity of base fluids increases when more nanoparticles are added to them. Numerous researchers have conducted investigations on the thermophysical characteristics of various hybrid nanofluids and their use as heat transfer fluids in diverse thermal systems. Using a water nanofluid based on multi-walled carbon nanotubes (MWCNTs) and graphene nanoplatelets, Hussein et al. [9] improved the thermal performance of a flat plate solar collector by 85% at a 4 LPM flow rate. Ekiciler et al. [10] conducted an analysis on the impact of hybrid nanofluid on the heat transfer efficiency of a parabolic concentric solar collector. The results of the study indicate that the Ag–MgO/Syltherm 800 hybrid nanofluid with a nanoparticle volume fraction of 4.0% is the optimal working fluid for the PTC receiver in terms of efficiency. Kazemian et al. [11] investigated the utilisation of four distinct hybrid nanofluids, namely MWCNT – Al_2O_3, MWCNT – SiC, Graphene – Al_2O_3, and Graphene – SiC, inside a photovoltaic – Thermal (PVT) solar collector and observed that the MWCNT-SiC nanofluid exhibited the best thermal efficiency of around 1.85% and electrical efficiency of 56.55%. The thermal characteristics of various volume concentrations of Al2O3/water, CuO/water, and Al_2O_3–CuO/water nanofluids were analysed by Gangadevi and Vinayagam [12] also investigated the effects of these nanofluids on PVT solar collectors. The findings of the study clearly demonstrate a positive correlation between volume concentration and thermal conductivity. This relationship ultimately results in improved thermal and electrical efficiencies of the photovoltaic-thermal (PVT) system, with an increase of 82% in thermal efficiency and 15% in electrical efficiency. While numerous studies using hybrid nanofluid

in PVT systems have been published in recent years, optimising the parameters to make the most efficient use of the system with minimal loss is still a priority. Hence, in this study, a Technique for Order Preference by Similarity to Ideal Solution (TOPSIS), Multi-Objective Optimization on the basis of Ratio Analysis (MOORA) Multi Criteria Decision Making (MCDM) tools used to optimize the parameters of PVT system with Al_2O_3 – CuO / water hybrid nanofluid.
The main goal of this paper is to select the suitable heat transfer fluid for PVT based hydrogen production system to generate more electrical power output and hydrogen yield rate. Furthermore, the results of the TOPSIS and MOORA techniques are validated with the experimental results.

1.1 Multi Criteria Decision Making (MCDM)

MCDM is a subfield of operations research that helps to ascertain the most optimum choice from a set of options based on various criteria. Benjamin Franklin created an algorithm based on the principles of moral algebra and then presented an approach for Multiple Criteria Decision Making (MCDM). There are five main parts to an MCDM model: (1) the objective, (2) the decision maker's preferences, (3) the alternatives, (4) the criteria, and (5) the outcome [13]. MCDM may be roughly categorised into two main branches, namely Multi Attribute Decision Making (MADM) and Multi Objective Decision Making (MODM). The steps followed in MCDM problem is presented in Fig. 1. Various MCDM approaches are now available and used in diverse applications, dependent upon the inherent characteristics of the decision issue. The list of frequently used MCDM techniques is given below.
1. Analytic Hierarchy Process (AHP)
2. Analytic Network Process (ANP)
3. Technique for Order of Preference by Similarity to Ideal Solution (TOPSIS)
4. Elimination and Choice Expressing Reality (ELECTRE)
5. Preference Ranking Organization METHod for Enrichment Evaluations (Promethee)
6. Vlsekriterijumski OptimizacijaI Kompromisno Resenje (VIKOR)
7. Multi-Objective Optimization method on the basis of Ratio Analysis (MOORA)

In this study, the optimal heat transfer fluids for improving the performance of a PVT-based hydrogen generation system were determined using the TOPSIS and MOORA methodologies.

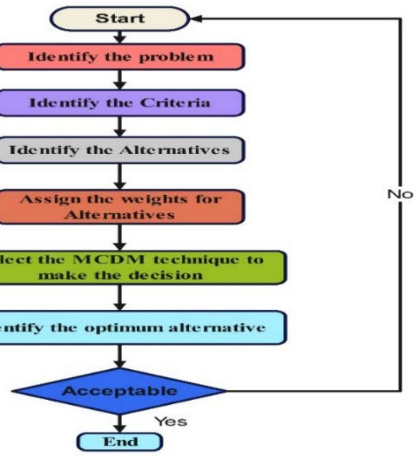

Fig.1 General Procedure of MCDM process

1.2 TOPSIS

TOPSIS is a kind of MCDM method that was introduced by Hwang and Yoon in 1981 [14]. In this approach, the most suitable choice was chosen by considering the minimal distance between the ideal positive solution and the maximal distance from the ideal negative solution. Due to its simplicity, versatility, and applicability to decision problems of varying scales, this strategy has been extensively used across several applications over the last few decades. The TOPSIS approach has been utilised by Chodha et al. to choose the robot for industrial welding applications [15]. In this method, Rank was determined using the TOPSIS approach, with weights determined using the entropy method. In order to determine the best setup for a hybrid hydrogen production system, Xu et al. [16] presented a two-stage MCDM strategy. The identification of Pareto solutions was accomplished via the use of the non-dominated sorting genetic algorithm (NSGA)-II. Subsequently, the weights and optimal solution were determined by using the CRITIC and TOPSIS methodologies. Nazari et al. [17] have used the TOPSIS approach to select the suitable site to install the Photovoltaic module. Podder et al. [18] investigated the ideal approach for achieving maximum performance via the use of the non-dominated sorting genetic algorithm (NSGA)-II and the TOPSIS technique. The findings showed that at an ideal mass flow rate of 0.02 kg/s, input temperature of 32 °C, and inclination angle of 38.88°, the thermal and electrical efficiencies reached 82.55% and 10.45%, respectively. The literature review revealed that few studies have utilised TOPSIS to determine PVT solar collector's ideal parameter. The TOPSIS method's stages are outlined below.

Step 1: The decision matrix developed for evaluating i options against j Criteria (PDC) will be presented in the order of ‘xij’ and given in (1). In this study, 30 sets of alternatives and 3 criteria were used to generate the decision matrix.

$$X_{ij} = \begin{bmatrix} X_{11}\ X_{12} \ldots\ldots\ldots\ldots X_{1j} \\ X_{21}\ X_{22} \ldots\ldots\ldots\ldots X_{2j} \\ . \\ . \\ . \\ X_{i1}\ X_{i2} \ldots\ldots\ldots\ldots X_{ij} \end{bmatrix} \qquad where\ i = 1,2,3......n \quad j = 1,2,3......n \tag{1}$$

Step 2 : The normalized decision matrix (Yij) was calculated by using the equation (2)

$$Y_{ij} = \frac{X_{ij}}{\sqrt{\sum_{i=1}^{n} X_{ij}^{2}}} \quad where\ i = 1,2,3......n \quad j = 1,2,3......n \tag{2}$$

Step 3: Weighted normalized matrix (Mij) was calculated by multiplying the weight (Wij) with Yij.

$$M_{ij} = W_{ij} \times Y_{ij} \qquad where\ i = 1,2,3......n \quad j = 1,2,3......n \tag{3}$$

Step 4: The ideal best and ideal worst solution was calculated by using the equations (4) and (5)

$$A^{+} = \left\{V_1^{+}, \ldots\ldots\ldots\ldots V_n^{+}\right\} = \left\{\left(\max_i v_{ij}, j \in J\right)\left(\max_i v_{ij}, j \in J^{'}\right)\right\}, \quad i = 1,2,.......n \tag{4}$$

$$A^{-} = \left\{V_1^{-}, \ldots\ldots\ldots\ldots V_n^{-}\right\} = \left\{\left(\min_i v_{ij}, j \in J\right)\left(\min_i v_{ij}, j \in J^{'}\right)\right\}, \quad i = 1,2,.......n \tag{5}$$

Step 5: Determine the Euclidian distance from the ideal best and worst values using the following formulas.

$$D_i^+ = \sqrt{\sum_{j=1}^{n}\left(V_{ij} - V_j^+\right)^2} \tag{6}$$

$$D_i^- = \sqrt{\sum_{j=1}^{n}\left(V_{ij} - V_j^-\right)^2} \tag{7}$$

Step 6: Finally, the closeness index was calculated by using the equation 8.

$$CI = \frac{D_i^-}{D_i^+ + D_i^-} \tag{8}$$

1.3 MOORA

Researcher Brauers developed the MOORA technique to solve the decision matrix issue. In the last several decades, it has seen widespread usage for decision making due to its mathematical simplicity and applicability across a wide variety of issues. In order to choose the most appropriate electric car for use in public transportation, Hamurcu and Eren [19] used MOORA and TOPSIS methodologies. Khorshidi et al. [20] used fuzzy MOORA method to select the suitable location for solar power plant. Sarkodie et al. [21] have used different MCDM approaches (CRITIC, COPRAS, TOPSIS and MOORA) to evaluate the different renewable energy sources in Ghana. Although there have been many publications published on MOORA MCDM in recent years, only few have focused on its application to PVT-based hydrogen generation systems. Hence in this study, MOORA technique was used to select the suitable heat transfer fluid to enhance the electrical efficiency and hydrogen yield rate. This approach is identical to the TOPSIS one in the first three steps (Equation 1, 2, and 3). Step 4 involves determining the assessment value by subtracting the total weights of all positive criteria from the total weights of all negative criteria. The mathematical equation for step 4 is given in equation 9.

$$Y_i = \sum_{j=1}^{k} M_{ij} - \sum_{j=k+1}^{P} M_{ij} \tag{9}$$

Where ‘k’ is the beneficial and ‘P’ is the non beneficial

2 Experimental Setup Description

In this study, the electrical efficiency, thermal efficiency, and hydrogen yield rate of a PVT-based hydrogen production system were analysed using a test rig consisting of three main components: 1. PVT system, 2. hydrogen generating system, and 3. Storage system. The pictorial view of the developed PVT system is depicted in Fig. 2. The PVT system consists of PV module, spiral flow thermal collector, heat transfer system and flow control devices. The electrolyzer was used in the hydrogen generation system to split the water into hydrogen and oxygen. The generated hydrogen and the required water to extract the heat from PV module are stored separately using the storage tanks. The experiment was conducted over a period of one week, starting at 7 AM and ending at 6 PM each day. Throughout this duration, the average measurements of solar radiation, PV module temperature, fluid outlet temperature, output voltage, and current were recorded and used for further computations.
During this study, four different nanofluids such as water, Al_2O_3/water, CuO/water Al_2O_3 - CuO/water nanofluid were used as a heat transfer fluid in thermal collector. The nanofluids were produced utilising a two-step preparation process, with volume concentrations of

0.05%, 0.1%, and 0.2%. The pictorial view of the prepared nanofluids are presented in Fig. 3.

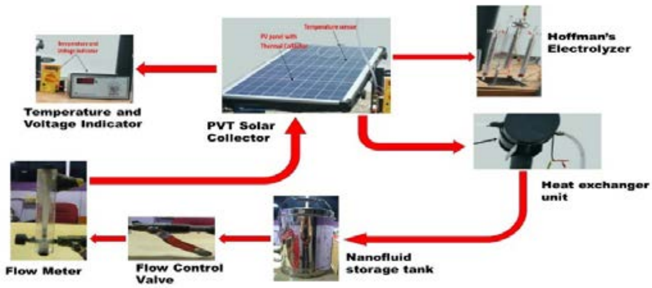

Fig. 2 Pictorial view of PVT solar collector based hydrogen production system

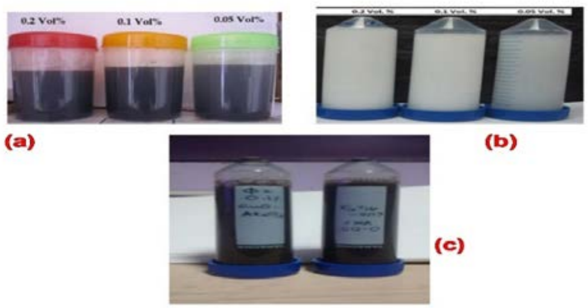

Fig. 3. Pictorial view of the prepared nanofluids (a) CuO /water nanofluid (b) Al_2O_3/water, and (c) Al_2O_3 - CuO/water (hybrid nanofluid)

3 Results and Discussions

3.1 Discussions on experimental results

The experimental test was carried out to investigate the PVT system performance with different volume concentrations of nanofluids. The nanofluids prepared with three different sonication times (2 hrs, 3 hrs and 4 hrs) were used and studied the electrical, thermal efficiency and hydrogen yield rate. The obtained values are summarized and presented in the Table 1. The variations of electrical efficiency, thermal efficiency and hydrogen yield rate of PVT system for different heat transfer fluids are presented in Fig. 4. The research findings firmly demonstrated that there was a positive correlation between the volume concentration, sonication time and the effectiveness of the thermal collector. For water and all nanofluids, the highest levels of thermal and electrical efficiency were reached around midday (12.00 Noon), and then gradually decreased until 4 p.m. generally, the hydrogen yield rate in the electrolyzed is mainly depends on the PV module electrical power output. Hence the maximum hydrogen yield rate is obtained at 12.00 noon for all the cases. On the other hand, the thermal conductivity of the nanofluid increases with increasing the concentration of nanoparticle in base fluid and sonication time. This leads to extract more heat from PV module and enhance the PV module power output. Hence the PVT system with 0.2% volume concentration cools PV module effectively and yields more hydrogen compared with other heat transfer fluids.

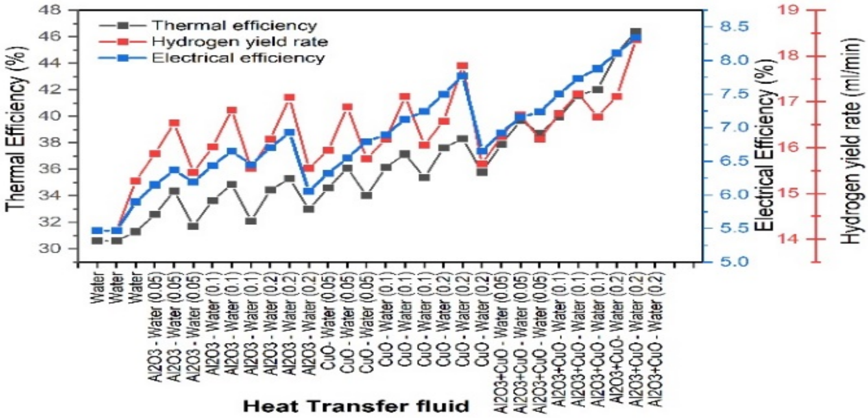

Fig. 4 Variations of Thermal efficiency, electrical efficiency and hydrogen yield rate for different heat transfer fluids

3.2 Discussions on TOPSIS and MOORA results

In this study, the suitable heat transfer fluid was selected to obtain maximum efficiency and hydrogen yield rate based on TOPSIS and MOORA MCDM methods. The required weights to calculate the values in the weighted normalized matrix was calculated by using Analytical Hierarchy Process method (AHP). Based on the results, the weights 0.5101, 0.0996 and 0.3901 were used in TOPSIS and MOORA methods. The results obtained by using the equations mentioned in the previous chapter (chapter 2) are summarized and given in Table 2. In this Table, the maximum assessment value (CI and Yi) is considered as best heat transfer fluid and minimum assessment value is considered as worst heat transfer fluid. Fig. 5 depicts the details of the rank obtained in TOPSIS and MOORA methods. Based on the results obtained in TOPSIS and MOORA methods, it can be noticed that the top 10 ranks are similar in both methods. But there are some rank changes notice in experiment number 10,12,14,15,16 and 19. The details of ranks and the corresponding assessment values are given in Table 3. Nearly 80% of the ranks obtained in both TOPSIS and MOORA methods are same. Hence the obtained decisions were compared with the experimental values. This comparison results also evident that maximum electrical, thermal efficiency and hydrogen yield rate were obtained for hybrid nanofluid with 0.2% volume concentration (rank 1). As a result, the hybrid nanofluid subjected to a 4-hour sonication period emerges as the most effective heat transfer fluid. During, high sonication time, the particles are dispersed uniformly in the base fluids and leads to enhance heat transfer rate effectively. The same kind of results also obtained in the previous study [22].

Tabel 1: Summary of experimental results

Exp. No	**Type of heat transfer Fluid**	**Nanoparticle volume concentration (%)**	**Sonication time (Hr)**	$\eta_{eletrical}$ **(%)**	$\eta_{Thermal}$ **(%)**	**Hydrogen yield rate (ml/min)**
1	Water	0	0	5.47	30.59	14.186
2	Water	0	0	5.47	30.59	14.186
3	Water	0	0	5.47	30.59	14.186
4	Al_2O_3 - Water	0.05	2	5.897	31.29	15.27
5	Al_2O_3 - Water	0.05	3	6.151	32.6	15.873
6	Al_2O_3 - Water	0.05	4	6.37	34.37	16.535
7	Al_2O_3 - Water	0.1	2	6.189	31.72	15.456
8	Al_2O_3 - Water	0.1	3	6.435	33.65	16.014
9	Al_2O_3 - Water	0.1	4	6.654	34.87	16.826
10	Al_2O_3 - Water	0.2	2	6.451	32.11	15.545
11	Al_2O_3 - Water	0.2	3	6.709	34.44	16.185
12	Al_2O_3 - Water	0.2	4	6.928	35.29	17.094
13	CuO - Water	0.05	2	6.055	32.98	15.545
14	CuO - Water	0.05	3	6.322	34.59	15.94
15	CuO - Water	0.05	4	6.551	36.09	16.885
16	CuO - Water	0.1	2	6.797	34.01	15.761
17	CuO - Water	0.1	3	6.898	36.15	16.185
18	CuO - Water	0.1	4	7.127	37.15	17.116
19	CuO - Water	0.2	2	7.244	35.38	16.059
20	CuO - Water	0.2	3	7.498	37.6	16.58
21	CuO - Water	0.2	4	7.773	38.31	17.794
22	Al2O3 +CuO - Water	0.05	2	6.654	35.79	15.642
23	Al_2O_3 +CuO - Water	0.05	3	6.925	37.88	16.245
24	Al_2O_3 +CuO - Water	0.05	4	7.157	39.66	16.714
25	Al_2O_3 +CuO - Water	0.1	2	7.233	38.74	16.178
26	Al_2O_3 +CuO - Water	0.1	3	7.504	39.94	16.744
27	Al_2O_3 +CuO - Water	0.1	4	7.733	41.58	17.176
28	Al_2O_3 +CuO - Water	0.2	2	7.879	42.03	16.677
29	Al_2O_3 +CuO - Water	0.2	3	8.11	44.75	17.124
30	Al_2O_3 +CuO - Water	0.2	4	8.339	46.4	18.359

Tabel 2: TOPSIS and MOORA method results

Exp. No	**Type of heat transfer Fluid**	**Normalized matrix**			**Weighted Normalized matrix**			**TOPSIS Method**				**MOORA method**	
								Di+	Di-	CI	Rank	Yi	Rank
1	Water	0.146	0.154	0.160	0.074	0.015	0.062	0.044	0.000	0.000	28	0.152	28
2	Water	0.146	0.154	0.160	0.074	0.015	0.062	0.044	0.000	0.000	28	0.152	28
3	Water	0.146	0.154	0.160	0.074	0.015	0.062	0.044	0.000	0.000	28	0.152	28
4	Al_2O_3 - Water (0.05)	0.157	0.158	0.172	0.080	0.016	0.067	0.037	0.008	0.170	27	0.163	27
5	Al_2O_3 - Water (0.05)	0.164	0.164	0.179	0.084	0.016	0.070	0.032	0.012	0.268	24	0.170	24
6	Al_2O_3 - Water (0.05)	0.170	0.173	0.186	0.087	0.017	0.073	0.029	0.016	0.360	20	0.177	20
7	Al_2O_3 - Water (0.1)	0.165	0.160	0.174	0.084	0.016	0.068	0.033	0.011	0.256	25	0.168	25
8	Al_2O_3 - Water (0.1)	0.172	0.169	0.180	0.088	0.017	0.070	0.029	0.015	0.351	21	0.175	21
9	Al_2O_3 - Water (0.1)	0.178	0.176	0.189	0.091	0.017	0.074	0.025	0.020	0.448	15	0.182	15
10	Al_2O_3 - Water (0.2)	0.172	0.162	0.175	0.088	0.016	0.068	0.029	0.015	0.333	22	0.172	23
11	Al_2O_3 - Water (0.2)	0.179	0.173	0.182	0.091	0.017	0.071	0.025	0.019	0.434	17	0.180	17
12	Al_2O_3 - Water (0.2)	0.185	0.178	0.192	0.094	0.018	0.075	0.021	0.024	0.533	12	0.187	11
13	CuO-Water (0.05)	0.162	0.166	0.175	0.082	0.017	0.068	0.034	0.010	0.227	26	0.167	26
14	CuO - Water (0.05)	0.169	0.174	0.179	0.086	0.017	0.070	0.030	0.014	0.319	23	0.173	22
15	CuO - Water (0.05)	0.175	0.182	0.190	0.089	0.018	0.074	0.026	0.019	0.426	18	0.181	16
16	CuO - Water (0.1)	0.181	0.171	0.177	0.093	0.017	0.069	0.025	0.019	0.440	16	0.179	18
17	CuO - Water (0.1)	0.184	0.182	0.182	0.094	0.018	0.071	0.022	0.022	0.490	14	0.183	14

18	CuO - Water (0.1)	0.190	0.187	0.193	0.097	0.019	0.075	0.018	0.026	0.593	8	0.191	8
19	CuO - Water (0.2)	0.146	0.154	0.160	0.074	0.015	0.062	0.044	0.000	0.000	11	0.187	12
20	CuO - Water (0.2)	0.146	0.154	0.160	0.074	0.015	0.062	0.044	0.000	0.000	7	0.194	7
21	CuO - Water (0.2)	0.146	0.154	0.160	0.074	0.015	0.062	0.044	0.000	0.000	3	0.203	3
22	Al_2O_3+CuO - Water (0.05)	0.157	0.158	0.172	0.080	0.016	0.067	0.037	0.008	0.170	19	0.177	19
23	Al_2O_3+CuO - Water (0.05)	0.164	0.164	0.179	0.084	0.016	0.070	0.032	0.012	0.268	13	0.185	13
24	Al_2O_3+CuO - Water (0.05)	0.170	0.173	0.186	0.087	0.017	0.073	0.029	0.016	0.360	9	0.191	9
25	Al_2O_3+CuO - Water (0.1)	0.165	0.160	0.174	0.084	0.016	0.068	0.033	0.011	0.256	10	0.189	10
26	Al_2O_3+CuO - Water (0.1)	0.172	0.169	0.180	0.088	0.017	0.070	0.029	0.015	0.351	6	0.196	6
27	Al_2O_3+CuO - Water (0.1)	0.178	0.176	0.189	0.091	0.017	0.074	0.025	0.020	0.448	5	0.202	5
28	Al_2O_3+CuO-Water (0.2)	0.172	0.162	0.175	0.088	0.016	0.068	0.029	0.015	0.333	4	0.202	4
29	Al_2O_3+CuO - Water (0.2)	0.179	0.173	0.182	0.091	0.017	0.071	0.025	0.019	0.434	2	0.208	2
30	Al_2O_3+CuO - Water (0.2)	0.222	0.233	0.206	0.113	0.023	0.080	0	0.043	1.000	1	0.217	1

Tabel 3: The variations of rank and the assessment values of TOPSIS and MOORA method

Experiment. No	TOPSIS Method		MOORA Method	
	Assessment value	Rank	Assessment value	Rank
10	0.33250	22	0.172167	23
12	0.53325	12	0.187055	11
14	0.31897	23	0.173389	22
15	0.42612	18	0.181407	16
16	0.44030	16	0.178779	18
19	0.57638	11	0.18686	12

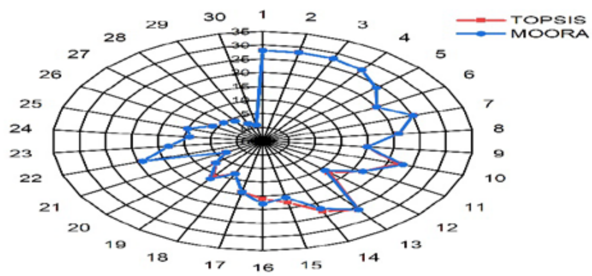

Fig. 5 The rank details of the TOPSIS and MOORA methods.

4 Conclusions

In this study, a different types of heat transfer fluids are used in PVT based hydrogen production system to enhance the performance of the system. Based on the previous study results, electrical efficiency, thermal efficiency and hydrogen yield rate are considered as a criteria for decision making and the weights are calculated using AHP method. The obtained results of this study are summarized below

1. The thermal conductivity of nanofluid increases with increasing the sonication time and volume concentration of nanofluids.
2. The maximum thermal efficiency, electrical efficiency and hydrogen yield rate are obtained for the PVT system with Al_2O_3 – CuO/water nanofluid with 0.2% volume concentration and 4 hrs sonication time.
3. Based on the obtained assessment value and rank in TOPSIS and MOORA method, nearly 80% of the ranks are same. And it is good agreement with the experimental results.
4. Top 3 rankings in both TOPSIS and MOORA were achieved by the Al2O3-CuO/water (0.2%- 4 hr sonication time), Al_2O_3-CuO/water (0.2%- 3 hr sonication time), and CuO/water (0.2%- 4 hr sonication time) combinations.

From the obtained results it can be concluded that the TOPSIS and MOORA MCDM methods can be used to select the best heat transfer fluid in PVT based hydrogen production system to enhance its performance. These findings might be valuable for researchers in conducting their investigations; nevertheless, more exploration of other methodologies may be necessary to arrive at a robust conclusion.

References

[1]. R. Agarwal, K. Verma, N.K. Agrawal, R.K. Duchaniya, and R. Singh, "Synthesis, characterization, thermal conductivity and sensitivity of CuO nanofluids," Applied Thermal Engineering, 102, 1024-1036, 2016. https://doi.org/10.1016/j.applthermaleng.2016.04.051

[2]. A. Aghanajafi, D. Toghraie, and B. Mehmandoust, "Numerical simulation of laminar forced convection of water-CuO nanofluid inside a triangular duct," Physica E: Low-dimensional Systems and Nanostructures, 85, 103-108, 2017. https://doi.org/10.1016/j.physe.2016.08.022

[3]. N.A. Usri, W.H. Azmi, R. Mamat, K.A. Hamid, and G. Najafi, "Thermal conductivity enhancement of Al_2O_3 nanofluid in ethylene glycol and water mixture," Energy Procedia, 79, 397-402, 2015. https://doi.org/10.1016/j.egypro.2015.11.509

[4]. M.F. Zawrah, R.M. Khattab, L.G. Girgis, H. El Daidamony, and R.E. Abdel Aziz, "Stability and electrical conductivity of water-base Al_2O_3 nanofluids for different applications," HBRC journal, 12 (3), 227-234, 2016. https://doi.org/10.1016/j.hbrcj.2014.12.001

[5]. S.Y. Jung, and H. Park, "Experimental investigation of heat transfer of Al_2O_3 nanofluid in a microchannel heat sink," International Journal of Heat and Mass Transfer, 179, 121729, 2021. https://doi.org/10.1016/j.ijheatmasstransfer.2021.121729

[6]. R.R. Sahoo, and V. Kumar, "Development of a new correlation to determine the viscosity of ternary hybrid nanofluid," International Communications in Heat and Mass Transfer, 111, 104451, 2020. https://doi.org/10.1016/j.icheatmasstransfer.2019.104451

[7]. M.H. Esfe, M.K. Amiri, and A. Alirezaie, "Thermal conductivity of a hybrid nanofluid" Journal of Thermal Analysis and Calorimetry, 134 (2), 1113-1122, 2018. https://doi.org/10.1007/s10973-017-6836-9

[8]. R.R. Sahoo, "Experimental study on the viscosity of hybrid nanofluid and development of a new correlation," Heat and Mass Transfer, 56, 3023-3033, 2020. https://doi.org/10.1007/s00231-020-02915-9

[9]. O.A. Hussein, K. Habib, A.S. Muhsan, R. Saidur, O.A. Alawi, and T.K. Ibrahim, "Thermal performance enhancement of a flat plate solar collector using hybrid nanofluid," Solar Energy, 204, 208-222, 2020. https://doi.org/10.1016/j.solener.2020.04.034

[10]. R. Ekiciler, K. Arslan, O. Turgut, and B. Kurşun, "Effect of hybrid nanofluid on heat transfer performance of parabolic trough solar collector receiver," Journal of Thermal Analysis and Calorimetry, 143, 1637-1654, 2021. 10.1007/s10973-020-09717-5

[11]. A. Kazemian, T. Salari, H. Ma, and Lu, "Application of hybrid nanofluids in a novel combined photovoltaic/thermal and solar collector system," Solar Energy,239, 102-116, 2022. https://doi.org/10.1016/j.solener.2022.04.016

[12]. R. Gangadevi, and B.K. Vinayagam, "Experimental determination of thermal conductivity and viscosity of different nanofluids and its effect on a hybrid solar collector," Journal of Thermal Analysis and Calorimetry, 136, 199-209, 2019. https://doi.org/10.1007/s10973-018-7840-4

[13]. J.R.S.C. Mateo, "Multi criteria analysis in the renewable energy industry" Springer Science & Business Media, 2012. https://doi.org/10.1007/978-1-4471-2346-0

[14]. C.L. Hwang, and K. Yoon, K, "Multiple attribute decision making: a state of the art survey," Lecture notes in economics and mathematical systems, 186, 58–191, 1981.

[15]. V. Chodha, R. Dubey, R. Kumar, S. Singh, and S. Kaur, "Selection of industrial arc welding robot with TOPSIS and Entropy MCDM techniques," Materials Today: Proceedings, 50, 709-715, 2022. https://doi.org/10.1016/j.matpr.2021.04.487

[16]. C. Xu, Y. Ke, Y. Li, H. Chu, and Y. Wu, "Data-driven configuration optimization of an off-grid wind/PV/hydrogen system based on modified NSGA-II and CRITIC-TOPSIS," Energy Conversion and Management, 215,112892, 2020. https://doi.org/10.1016/j.enconman.2020.112892

[17]. M.A. Nazari, A. Aslani, and R. Ghasempour, "Analysis of solar farm site selection based on TOPSIS approach," International Journal of Social Ecology and Sustainable Development (IJSESD), 9 (1), 12-25, 2018. DOI: 10.4018/IJSESD.2018010102

[18]. B. Podder, A. Biswas, and S. Saha, "Multi-objective optimization of a small sized solar PV-T water collector using controlled elitist NSGA-II coupled with TOPSIS," Solar Energy, 230, 688-702, 2021. https://doi.org/10.1016/j.solener.2021.10.078

[19]. M. Hamurcu, M. and T. Eren, "Applications of the MOORA and TOPSIS methods for decision of electric vehicles in public transportation technology," Transport, 37 (4), 251-263, 2022. https://doi.org/10.3846/transport.2022.17783

[20]. M. Khorshidi, B. Erkayman, Ö. Albayrak, R. Kılıç, and H.I. Demir, H.İ, "Solar power plant location selection using integrated fuzzy DEMATEL and fuzzy MOORA method," International Journal of Ambient Energy, , 43 (1), 7400-7409, 2022. https://doi.org/10.1080/01430750.2022.2068067

[21]. W.O. Sarkodie, E.A. Ofosu, and B.C. Ampimah, Decision optimization techniques for evaluating renewable energy resources for power generation in Ghana: MCDM approach, Energy Reports, 8, 3504-13513, 2022. https://doi.org/10.1016/j.egyr.2022.10.120

[22]. G. Rajendiran, G, V.B. Kuppusamy, and S. Shanmugasundaram, Experimental investigation of the effects of sonication time and volume concentration on the performance of PVT solar collector, IET Renewable Power Generation, 12(12), 1375-1381, 2018. https://doi.org/10.1049/iet-rpg.2018.5283